

Semiconductor gamma radiation detectors: band structure effects in energy resolution

Arsen Subashiev and Serge Luryi

Dept. of Electrical Computer Engineering, State University of New York at Stony Brook, Stony Brook, NY 11794-2350, U.S.A.

1. Introduction

Energy spectroscopy in semiconductor γ -detectors is based on registration of the total number of electron-hole pairs produced by a single γ -photon after a cascade of various processes. These include Compton scattering events, photo-absorption, deep core level excitation, core vacancy relaxation, emission of plasmons by the secondary electrons (holes), plasmon decay into electron-hole ($e-h$) pairs and impact ionizations. At each stage the cascade is accompanied by sequential energy branching between secondary particles, which results in almost random energy distribution in a cloud of secondary electrons and holes in the final state. The branching is terminated when the energy of a secondary electron or hole is below the impact ionization threshold. Importantly, to a very high precision and in a broad energy range, the number of created pairs N is just proportional to the initial energy $E = h\nu$, of the γ -photon, $N = E/\varepsilon$, where ε is the average excitation energy of a single pair (referred to as the pair excitation energy). For semiconductor materials the pair excitation energy ε is about $3E_g$, where E_g is the band gap energy and is typically about $2E_m$, i.e. twice the minimal energy required for electron to produce a pair by impact ionization in a process with momentum conservation. This means that electrons and holes possess a large average residual kinetic energy after cascade termination.

Due to the almost random nature of the cascade energy branching, the pair number N fluctuates from one event to the other. Therefore, the theoretical limit for the γ -detector energy resolution depends on the variance of the registered energy E , i.e. $\langle \delta E^2 \rangle = \langle \delta N^2 \rangle \varepsilon^2$. The variance differs from the Poissonian statistics by a factor F , called the Fano factor¹, so that $\langle \delta N^2 \rangle = F \langle N \rangle$. Experimental data for F are most reliably determined for Ge and Si where they are close to 0.1. For many years the statistical limitations of energy resolution expressed by the factor F were less important than those due to electronic noise and the effects of incomplete charge collection. However, owing to recent progress in electronics² and the development of pixel detectors³ the intrinsic contribution to energy resolution has become tangible. Moreover, a number of novel detectors, based on new energy-measurement principles (such as the Compton telescope^{4,5}) and new semiconductor materials⁶ are explored. Therefore, critical evaluation of the Fano factor theory becomes important in the search for materials with improved energy resolution.

Theoretical models used for Fano factor calculations have been based on widely varying assumptions, often ignoring the important details of the energy branching process.^{7,8} Therefore, the confidence in these models is questionable even though they routinely produce estimates of F in the range 0.06 to 0.14, close to the experimental results for a number of semiconductors.⁷ In this chapter, we overview some of the popular models used and discuss the most subtle aspect of energy branching, namely the pair correlations in the final-state energy distribution. We show that these correlations need being taken into account and that moreover they can be used in the search for materials with reduced Fano factor and hence improved intrinsic energy resolution.

2. Final state models

The pair production in semiconductor γ -detectors occurs by an ionization cascade that goes through a number of intermediate stages where the energies of secondary electrons or holes are much larger than the ionization energy. The relative energy loss at these stages is typically much smaller than the energy spread in the final state, as has been shown by Monte-Carlo modeling,^{9,10} using fairly well known cross-sections of elementary processes. For secondary high-energy electrons the dominant energy-loss process for high-energy electrons is the emission of plasmons (collective valence-band excitations).^{7,11} The density of valence-band electrons is almost the same for all tetrahedral semiconductors and the plasmon energy is close to 16 eV for Ge, Si, and A_3B_5 semiconductors. De-excitation of the deep core state vacancies goes through fluorescence or Auger-like Coster-Kronig transitions, also creating intermediate electrons and holes, spread in a wide energy interval in the conduction and valence bands, respectively.

The final stage of the energy branching is governed by a competition between the processes of impact ionization and phonon emission. The energy conservation in impact ionization for an electron with energy E_e reads $E_e = E_g + E_{1e} + E_{2e} + E_h$, where E_{1e} , E_{2e} , E_h are the kinetic energies of carriers (in this example, two electrons and a hole, respectively). Similar relation holds for impact initiated by a hole. After the bandgap is subtracted, the residual energy is distributed between 3 particles. The cascade process is repeated until the final energy of a secondary particle is smaller than the impact ionization threshold or until subsequent phonon emission becomes more probable. Termination of the cascade fixes the number N of pairs, since the excess energy dissipates without changing the particle number.

The most popular statistical approach to the Fano factor evaluation is based on the analysis of the energy distribution in the system of e - h pairs and phonons in the *final state*, i.e. at the stage when further creation of e - h pairs is impossible.

Consider the simplest case when phonon emission is not important. In this case, for a particular realization of the cascade process, the initial energy E is distributed between N pairs, $E = \sum E_i$, where E_i is the energy of the i -th pair. In this distribution the sum E is fixed, whereas the number of terms N is the statistical variable. It is instructive, however, to begin with the opposite situation with a sum of a fixed number N of independent random variables E_i , whose distribution is characterized by a mean $\varepsilon = \langle E_i \rangle$ and a variance $\langle \delta \varepsilon^2 \rangle = \langle E_i^2 \rangle - \varepsilon^2$.

In this case, according to the central limit theorem, the sum E will be normally distributed about its mean value $N\varepsilon$

$$P(E) = C_N \exp \left[-\frac{(E - N\varepsilon)^2}{2N\langle \delta\varepsilon^2 \rangle} \right], \quad (1)$$

where C_N is a normalization constant. For the case we are interested in, when the total (initial) energy is fixed for all events, while the number of pairs fluctuates from one realization of energy branching to another, we can re-interpret (1) to provide the probability distribution for N , viz.

$$P(N) = C \exp \left[-\frac{(N - \langle N \rangle)^2 \varepsilon^2}{2\langle N \rangle \langle \delta\varepsilon^2 \rangle} \right], \quad (2)$$

where C is another normalization constant; we have replaced N by $\langle N \rangle$ in the denominator since their difference is small. It is evident from Eq. (2) that the variance in the particle number is not Poissonian and that the Fano factor equals

$$F = \frac{\langle \delta\varepsilon^2 \rangle}{\varepsilon^2} \quad (3)$$

The above argument leading to the widely used expression (3) for the Fano factor can be illustrated by the so-called “shot-glass” model.¹² In this model, the initial energy E deposited in the semiconductor is taken analogous to the volume of water in a bathtub, while the electron-hole pair creation energy is represented by a volume of a shot glass with the help of which the tub is emptied sequentially. The shots are thought of being filled differently in a random fashion with a known mean and variance. The total number of shots used to empty the tub will fluctuate from one realization to another and one can apply the above reasoning leading to Eq. (3). The shot-glass model is an example of the class of uncorrelated models, called the *final-state models*. It assumes that the final state is formed as a composition of uncorrelated random events described by the parameters (mean and variance) of the single-event statistics, with no correlations between the events. The apparent non-Poissonian statistics in the final-state models results from one single constrain: the fixed total initial energy. As a result, Eq. (3) readily provides smaller than unity values for the Fano factor.

Equation (3) can be generalized to include “inelastic energy losses,” such as phonon emission. The energy loss associated with phonon emission is much lower than the ionization threshold. Phonon emission rate is also much lower than that of impact ionization, except very near the threshold where the ionization rate is much reduced. Near the threshold, the emission of a single phonon can make the next impact ionization impossible. The apparent shift of the ionization threshold can be accounted for by an adjusted value of ε . In the final state models these events are assumed independent so that fluctuations of the phonon energy losses are additive to those in E_i . The modified Eq. (3) is then of the form

$$F = \frac{\langle \delta\varepsilon^2 \rangle + (\hbar\omega)^2 \rho_{ph}}{\varepsilon^2}, \quad (4)$$

where ρ_{ph} is the average number of phonons emitted per e - h pair (created before the cascade termination). The number of emitted phonons is assumed to have Poissonian statistics. The average final-state pair energy is $\varepsilon = E_g + \langle K_e \rangle + \langle K_h \rangle$, where K_e and K_h are the kinetic energies of electrons and holes, distributed in a range from zero to the impact ionization threshold E_{th} . The number of phonons emitted before cascade termination is small and so are the corresponding energy losses, $\hbar\omega\rho_{\text{ph}} \ll \varepsilon N$ (similarly small energy losses come from other inelastic processes, such as fluorescence of deep-level holes, bremsstrahlung emission with some radiation escape from the crystal, etc.).

In order to use Eq. (4), one needs to know or assume the energy distribution in the final state. The simplest assumption is that final-state electrons are distributed in p -space homogeneously with a parabolic energy band spectrum.¹³ This implies a distribution proportional to the band density of states (DOS) and cut at E_{th} . For this distribution, the average pair kinetic energy $\langle K_e \rangle + \langle K_h \rangle = 1.2 E_m$, where E_m is a maximum allowed energy equal to the ionization energy threshold, $E_m = 1.5 E_g$. Then, the average energy needed for a pair production appears to be equal $\varepsilon = E_g + 1.2E_m = 2.8 E_g$, which is close to experimental data. Calculations of $\langle \delta\varepsilon^2 \rangle$ (with the same assumption of homogeneously distributed final-state particles in p -space up to the energy of $3/2 E_g$) give $2 \langle (\delta K_i)^2 \rangle = 9/2 \times 0.07 E_g^2 = 0.315 E_g^2$. This gives the value $F \approx 0.04$ to the electronic contribution to the Fano factor, which is far below the experimental data. To obtain a Fano factor that is closer to experiment (at least two times larger), one either has to assume an unrealistically large phonon contribution or to find other channels of energy loss. Thus, in order to obtain good agreement with the experimental data for Ge, the author of a widely cited paper¹⁴ assumed the energies of electrons and holes spread over half of the conduction and valence band, respectively, while the densities of states were assumed constant. The author of a well-known book² assumes that the total number n of phonons emitted in the pair production (this number is $n = E - NE_g$) fluctuates according to the Poisson statistics. This assumption (also yielding $F < 1$) has no sound justification and leads to a strong dependence of the Fano factor on the phonon energy. For most semiconductors it overestimates the value of F (compared to experiment). Other authors¹⁵ calculated the average number of phonons emitted before the cascade termination and thus estimated the average phonon energy loss as a function of initial electronic energy, which represents the second term in Eq. (4). However, their approximate approach used to evaluate the energy distribution function (now extending far beyond the impact ionization threshold) also required to adjust the bandgap to obtain reasonable values of Fano factor and pair excitation energy.

Within the final-state model framework, the phonon losses are statistically independent and should be treated as simply additive in calculations of the average excitation energy and the Fano factor. For only a few emitted phonons per pair, the phonon contribution is rather negligible. Microscopic consideration of energy branching readily suggests that the main effect of phonon emission is a strong shift of the impact ionization threshold, and thus the increase of the width of the kinetic

energy distribution. This affects both the average excitation energy and the Fano factor, even when the average number of emitted phonons is small.

This review of the final-state model approach is prompted by a recent paper,¹² which asserts that the model “provides a convenient framework for and point of departure for analyzing the essential statistical features of microscopic theories”.

It is clear that usefulness of final-state models is limited by the need to make assumptions about the final state distribution that go beyond the model itself. As a result, these models may often be misleading since the key assumptions, such as the role of phonon losses, may not be justified.

Nevertheless, it is important to examine the final-state model approach *on its principle*, leaving aside all uncertainties in the additional assumptions. This has been done in our recent paper¹⁶ on the basis of an exactly soluble model of sequential energy branching. In this model, called the random parking problem, one can calculate exactly both the Fano factor and its representation by the final-state model. This approach has elucidated the principal drawback of the latter.

The problem with all final-state models is that they postulate statistically independent final-state pair energies. This leads to the Gaussian distribution (1) and further to Eq. (3)]. However, the kinetics of an ionization cascade produces a *correlated* energy distribution in the final state, so that for a pair of electrons in the final state with energies E_i and E_j one has $\langle (E_i - \varepsilon) (E_j - \varepsilon) \rangle \neq \delta_{ij} (\langle E_i \rangle^2 - \varepsilon^2)$. Correlations between different terms in $E = \sum E_i$ invalidate Eqs. (1) and (3), whose derivation was based on the central limit theorem.

The importance of correlations can be easily illustrated in the shot-glass model: imagine that the man with the shot-glass watches what he is doing and compensates for an underfilled shot by following it with a shot with more than average filling, so that two successive glasses together scoop the same amount of water. Evidently, the fluctuations will be strongly reduced compared to predictions of Eq. (3). One can observe that this type of correlations is typical for energy branching: e.g., the division of initial energy between two particles produces a state where small energy of one particle is paired with large energy of the other. We shall discuss these correlations further and show that they are of major importance at the final stage of the energy branching.

Another relevant observation that follows from our exact model analysis¹⁶ is the importance of the *shape* of final energy distribution. It turns out that the exact one-particle distribution has a narrow peak at small energies. Therefore, combined with exact statistics, Eq. (3) will always predict a lower bound estimate for F .

3. Kinetics of energy branching: one-particle distribution function

For a realistic band structure, phonon spectrum, and scattering matrix elements, the calculations are necessarily numerical. To analyze qualitative features, we discuss a kinetic approach to the distribution function and present analytical results for a simplified model, where the valence band is so narrow, that one can neglect the kinetic energy of created hole. In this case the energy at the every stage of the cascade is distributed between the two secondary electrons. This case and some of its generalizations permit of an analytical solution.^{14,15,17}

Correlations in sequential energy branching are fully included in the so-called “crazy carpentry” (CC) model due to van Roosbroeck.¹⁷ It illustrates the branching process by random cutting of a wooden board into two pieces with the removal of a unit-length board from one piece (if its length is less than unity, the piece is discarded). The removed unit boards are stored and the process is repeated discarding all lengths less than unity until the entire board is used up. The initial board length is associated with the incident energy and the number of stored unit-length boards with the number of e-h pairs produced in the sequential energy branching. The discarded pieces represent the residual kinetic energies of electrons and holes in the final state.

An alternative but perhaps more transparent illustration of sequential energy branching is the so-called “random parking problem” (RPP). It is equivalent to the CC model¹⁷ and leads to the same equations and analytical results. In this model one studies the distribution of cars of unit size in a long linear parking lot, assuming that they arrive sequentially in time at random position in the lot. A car is rejected if it lands at an occupied space. The process is terminated when the so-called “*jamming limit*” is achieved, i.e. when all remaining gaps between the cars do not exceed unit length. The energy branching can be considered in terms of the RPP if one identifies the incident particle kinetic energy with the parking lot length and the pair creation energy with the car size. The quantities of interest are the filling factor (average number of cars per unit length), equivalent to the average pair excitation energy, and the fluctuation of the number of cars in different realizations that can be represented by the Fano factor. A number of generalized RPP problems have been studied, including the model of cars shrinking after they are parked¹⁸ that describes the case when the minimum pair creation energy is larger than the band gap (the energy removed from the system in pair creation), and the two-size parking problem¹⁹ that models the semiconductor with several minima in the conduction band (resulting in several impact ionization thresholds).

The key distinction of the CC and RPP models from the final-state models is the account of *sequential* energy branching that leads to correlations in the final distribution. In contrast, the final state models sample the energy repeatedly in an uncorrelated fashion.¹² Nevertheless, application of the CC and RPP models to sequential energy branching in radiation detectors was viewed with some suspicion. The early calculations (including Monte-Carlo modeling) of the excitation energy and the Fano factor had led to the belief that reliable results require an almost infinitely long parking lot (corresponding to very high initial energy, at least $E_0 > 100E_g$). At these high energies, processes other than impact ionization (e.g., plasmon emission, deep core electron excitation and so on) make the energy distribution between the secondaries highly inhomogeneous. This would render the results meaningless.¹² However, we have shown^{18,19} that the recursion division process saturates at a much earlier stage of initial energies, $E_0 \approx 7$ to $10 E_g$, after which the results become insensitive to the initial energy distribution. It was also shown^{18,19} that the recursive and the kinetic approaches are equivalent in the limit of infinitely high initial energy.

In this section, we consider kinetic evolution of the one-particle distribution function in the RPP model of sequential energy branching with a *finite* initial energy. Having obtained the exact single-particle distribution in the jamming limit, we then calculate the average excitation energy and the Fano factor using Eq. (3).

The kinetic equation for the electron energy distribution function $f(E)$ can be written in the form

$$\frac{\partial f(E,t)}{\partial t} = -R(E)f(E,t) + d \int_{E+E_0}^{E_0} dE' \rho(E') P(E',E) f(E',t) \quad , \quad (5)$$

where $R(E)$ is the impact ionization rate for an electron with initial energy E and $P(E',E)$ is the probability of an impact ionization process with initial energy E' and final electron energy E . The DOS function $\rho(E)$ is for initial states. The second term of Eq. (5) describes electron ionization resulting in a new electron in the state with energy E .

The factor d represents the degeneracy of the branching by impact ionization. For a narrow valence band, there are $d = 2$ final states with the same final energy of electrons; for a model with symmetrical conduction and valence bands, $d = 3$. In the RPP model, the function $f(E,t)$ represents the distribution of gaps between cars at the moment t . The same new spacing can evidently be obtained either on the right or on the left side of the newly arrived car.

Kinetic equation (5) describes the evolution of the energy distribution in the branching cascade and evidently, it does not conserve the number of particles. However, it is consistent with the total energy conservation law in a form

$$\int_0^\infty \left(E + \frac{E_{\text{th}}}{d-1} \right) f(E,t) \rho(E) dE = E_0 + \frac{E_{\text{th}}}{d-1} \quad . \quad (6)$$

Multiplying Eq. (5) by $[E + E_{\text{th}}/(d-1)]\rho(E)$, integrating it over energy and using Eq. (6), one can find $R(E)$ for any given $P(E',E)$. Equation (5) should be solved with the initial condition $f(E,t=0) = C \delta(E-E_0)$ for the branching process initiated by a high-energy electron created by the initial Compton event; constant C can be easily found from (6), $C = \rho^{-1}(E_0)$. Next, the number of pairs is given by

$$N_p = \frac{1}{d-1} \left[\int_0^\infty f(E,t) \rho(E) dE - 1 \right] \quad , \quad (7)$$

so that the pair excitation energy equals

$$\varepsilon = N_p^{-1} \left(E_0 + \frac{E_{\text{th}}}{d-1} \right) \quad (8)$$

Equation (8) may seem to be at variance with the former definition of the pair excitation energy. But that definition referred to the limit $N_p \gg 1$, where the additional term in Eq. (8) is negligible. For finite and especially the intermediate

stage of energy branching with E_0 in the range of 3 to 5 E_{th} , this correction ensures the linear growth with energy of the number of created pairs.

To study the kinetics of the energy branching, it is convenient to use the Laplace transformation in time,

$$F(E, p) = \int_0^{\infty} e^{-pt} f(E, t) dt . \quad (6)$$

Applied to Eq. (5) this gives

$$pF(E, p) = -R(E - E_{th})F(E, p) + d \int_{E+E_{th}}^{\infty} P(E', E)F(E', p)\rho(E')dE' + f(E, 0) . \quad (7)$$

Two important observations are in order. First, Eq. (7) can be used for any initial energy E_0 of the particle initiating the cascade process. Second, the Laplace transform function $F(E, p)$ is expressed through $F(E+E_{th}, p)$ and therefore it can be found recursively, starting from the energy range $E_0 - E_{th}$ and then going down to lower energies. For the case of the narrow valence band, the temporal evolution of normalized energy distributions,

$$f^*(E, t) = \frac{f(E, t)}{E_0 + E_{th} / (d - 1)} , \quad (8)$$

is shown in Fig. 1. Note the rapid decay of the high-energy tail of the distribution and growth of the peak near zero. This peak in the population of low-energy states leads to the underestimation of the Fano factor by the final-state model.

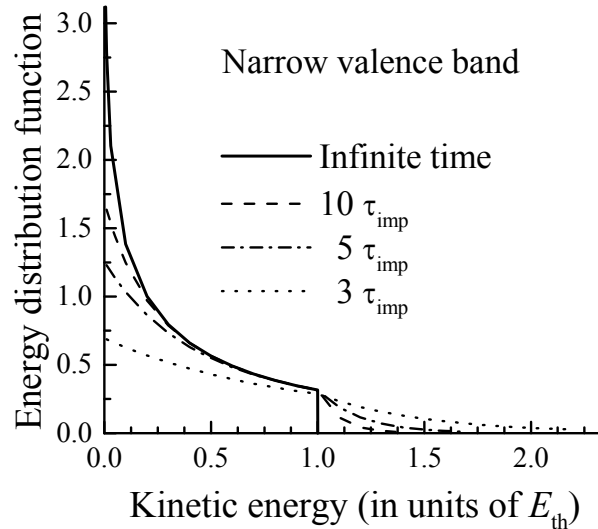


Figure 1. Evolution of the energy | distribution function of electron in case of a narrow valence band from initial state with one particle with energy 20 E_{th} .

The final distribution can be easily obtained using the Heaviside expansion theorem for the Laplace transforms, which gives

$$f(E, t \rightarrow \infty) = d \int_{E+E_{th}}^{\infty} P(E') F(E', 0) \rho(E) dE', \quad 0 < E < E_{th}. \quad (8)$$

Here $F(E', 0)$ is the solution of Eq. (7) at $p = 0$, viz.

$$F(E, 0) = R(E - E_{th})^{-1} d \int_{E+E_{th}}^{\infty} P(E') F(E', 0) \rho(E') dE' + f(E, 0) \quad (9)$$

Next, we trace the convergence of the distribution to its limiting form with the increase of E_0 . For a narrow valence band, the distribution function for $E_0 \rightarrow \infty$ is known from the solution of the RPP with an infinitely large parking lot and is of the form

$$f^*(E, t \rightarrow \infty) = 2 \int_0^{\infty} s e^{-Es - 2I(s)} ds, \quad (10)$$

where $f^*(E) = f(E)/E_0$ (with $E_0 \rightarrow \infty$) is the normalized distribution function, and

$$I(s) = \int_0^s \frac{1 - e^{-u}}{u} du. \quad (11)$$

The normalized distribution function $f^*(E, t \rightarrow \infty)$ calculated for several initial energies E_0 are shown in Fig. 2.

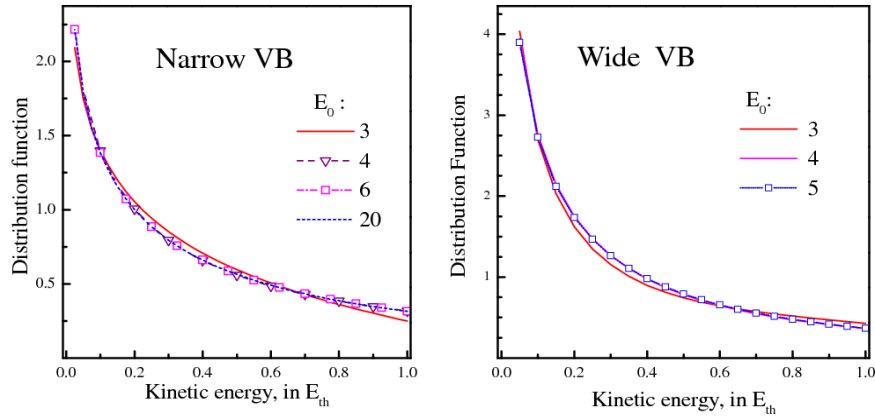


Figure 2. Average (over realizations) one-particle kinetic energy distribution functions after the energy branching termination. Different lines correspond to different initial particle energy E_0 (in units of E_{th}).

As the initial energy increases, one can observe a very rapid convergence of the distribution to its final form corresponding to $E_0 \rightarrow \infty$. To within 1%, the results become indistinguishable already with $E_0 = 4E_{th}$.

The obtained distribution functions are precise enough for the calculations of the average kinetic energy and the number of pairs in the final state (and thus both the pair excitation energy and its variance).

Similar analysis can be done for a finite-width valence band (see the right panel of Fig. 2). The rapid convergence is again in evidence. This convergence, found to be a general property of the branching process,^{18,19} leads to an important conclusion: details of energy branching at the initial and intermediate stages are not important for the final state energy distribution, since they do not produce an excessive number of particles with small energy. Further averaging over the distribution of secondaries in the intermediate stages has no influence on the final distribution and hence on the energy resolution.

This conclusion is very important for the energy branching problem and deserves to be further illustrated by the RPP model and formulated more accurately. Suppose at the initial stages of filling the parking line the cars are trying to observe some rules, say, try to park regularly at a distance $N_1 E_{th}$. Our conclusion is that the effect of this strong ordering on the final distribution function will be precisely described as

$$f_c(E) = f(E) \left(1 + \frac{1}{N_1} \right), \quad (12)$$

where $f_c(E)$ is the final state distribution function for the correlated parking, since the normalized distribution function $f^*(E)$ remains exactly the same. The only effect of correlation is some increase of the number of particles in the final state that can be taken into account.

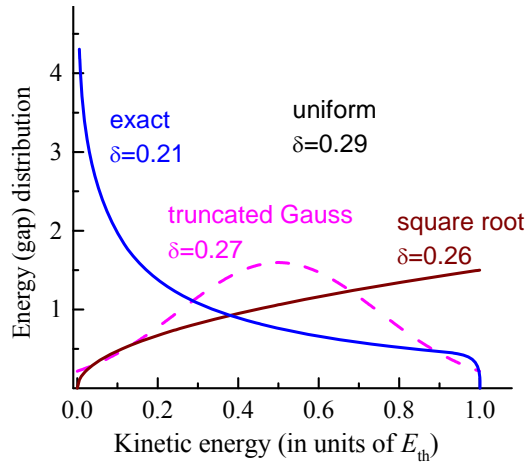


Figure 3. Comparison of the distribution functions used in different final state models together with corresponding mean square deviations for the case of a narrow valence band.

Figure 3 compares several model final-state distribution functions used in the literature.^{13,14} Also shown is the mean square root deviation δ for each model. In terms of δ , the final-state model estimate of the Fano factor is $F = \delta^2$.

One can observe that even though all final-state models predict values of the Fano factor below 0.1, their prediction capability is limited. Most significant is the fact that the exact one-particle distribution function gives the final-state (uncorrelated) value of the RPP Fano factor as $F_{\text{unc}} = 0.044$, whereas the exact value of the Fano factor for RPP model is known¹⁶ to be $F = 0.051$. Calculations based on the exact two-gap distribution function, taking into account correlations between *nearest-neighbor gaps only*, produce a correction to F_{unc} that brings F very close to the exact value.¹⁶ This means that correlations between distant gaps are not as important as the nearest-neighbor correlations.

4. Two particle correlations and Fano factor energy dependence

The noted drawback of the final-state models is the assumption of uncorrelated energy distribution between the secondary particles in the final state. To further elucidate this point, we return to the narrow valence band model represented by RPP. In this model, the residual energy of pair creation is distributed between two secondary electrons. Consider now a special case of random parking on a lot whose length is triple the size of a single car, see Fig 4. One can readily see that *two* cars will always park in this lot, with no fluctuation of this number (the unique case of three tightly parked cars with no gaps has zero probability). Accordingly, when in a random sequence of energy branching a particle of energy equal to $3 E_{\text{th}}$ is created, the next energy branching will produce exactly 2 particles with no fluctuation, irrespectively of the fluctuating kinetic energies of these particles. When the initial energy is close to $3 E_{\text{th}}$, the 2-particle final state will dominate. Correlations of this type will have an influence on the fluctuations of the final number of particles in all cases when at intermediate stage one of the created secondaries has a small energy. This clearly compromises the validity of Eq. (3). In principle, one can take such correlations into account in the kinetic approach. One needs to study the kinetics of the fluctuations of the distribution function, in such a way that the source of these fluctuations is itself modified by the correlations in the energy distribution.²¹ This approach is involved mathematically and has not yet been developed in full.



Figure 4. Random parking on a line $L = 3$. Two cars are always able to park, while three cars can never do it. Therefore, even though the spacing between cars fluctuates, there are no fluctuations of the number of cars.

Next, we consider the *recursive* approach, which is another purely statistical technique, specifically developed for branching processes. It studies the moments of the final-state energy distribution as functions of the initial energy. Due to the

self-averaging properties of the branching process, the moments of distribution for the state emerging from high values of the initial particle energy can be recursively evaluated through the moments of the distribution for smaller initial energy. The recursive equations for the RPP were first derived by Rényi²² and applied to the energy branching problem by van Roosbroek.¹⁷

The structure of recursive equations can be nicely illustrated in the RPP model. Consider the mean square of the number of cars placed along a line of length L . If there is a car at a distance x from the left end of the line, then the whole line is divided by this car into two lines of lengths x and $L-x-1$. The average $\langle N^2(L) \rangle$ can then be written in the form

$$\langle N^2(L) \rangle = \langle [1 + N(x) + N(L-x-1)]^2 \rangle. \quad (12)$$

Here the average is taken not only over all realizations of branching for the intervals x and $L-x-1$ but also over the variation of x in the range $0 < x < L-1$. Since both the left and the right sides of this division are equivalent, we find

$$\langle N^2(L) \rangle = 1 + 2\langle N(x)^2 \rangle + 4\langle N(x) \rangle + 2\langle N(x)N(L-x-1) \rangle. \quad (13)$$

The last term in (13) correlates the number of cars that will be subsequently placed in the intervals x and $L-x-1$. This correlation is negligible for large L and x , but it is important for small L , x and thus affects the resulting value of the Fano factor. Equation (13) should be accompanied by an equation for the mean $\langle N(L) \rangle$, which by the same reasoning is of the form

$$\langle N(L) \rangle = \langle 1 + N(x) + N(L-x-1) \rangle = 1 + 2\langle N(x) \rangle. \quad (14)$$

Due to the uncorrelated nature of the branching itself, one can use the solution of Eq. (14) to calculate the correlation function in (13). We obtain

$$\langle \delta N^2(L) \rangle = 2\langle N(x)^2 \rangle + 2\langle N(x)N(L-x-1) \rangle - 4\langle N(x) \rangle^2, \quad (15)$$

Note that all terms in the right-hand side of Eq. (15) are of the order of N^2 but their difference is of the order of N . The correlation effects are therefore not negligible and sufficient accuracy is required in calculations. For the case of RPP and for several generalized RPP models, exact solutions of Eqs. (13-15) can be obtained^{18,19,22} using Laplace transformation of the recursive equations, which leads to differential equations for the Laplace transforms. These solutions are helpful in assessing the errors introduced by various approximations.

We have applied the statistical recursive approach to the calculation of the particle number fluctuations in the energy branching problem, considering the cases of a narrow valence band, symmetric (parabolic) bands, bands with constant DOS, and the case when the valence band has a finite energy.

The kinetic energy variance is shown in Fig. 5 as function of the initial particle energy (which is needed for calculations of the Fano factor). For large $E_0 > 6 E_{th}$ the variance grows linearly with E_0 , which manifests the sub-Poissonian statistics

with a constant Fano factor. For small $E_0 < 6 E_{th}$ one see a strong variation of the variance indicating the importance of correlation effects. For the narrow valence band the variance goes to zero at $E_0 = 3 E_{th}$, as discussed above. A dip in the variance near $3 E_{th}$ remains also in the wide valence band model, although the effect there is less pronounced.

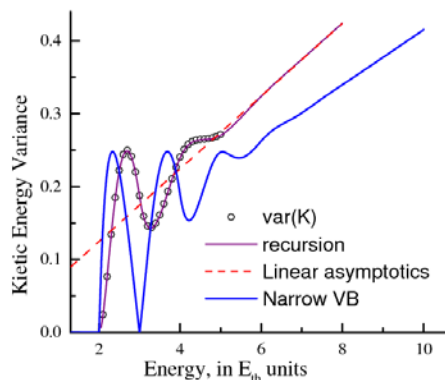


Figure 5. Dependence of the kinetic energy variance on the initial energy for a model with two symmetrical bands (dots on a line) and also for the case of a narrow valence band.

All exactly solvable models indicate the insensitivity of the results to the initial distribution for large energies, starting with $E > 5 E_{th}$. This makes the recursive approach eminently tractable, even using realistic branching models. In the small range of energies where the results are sensitive to the initial distribution, one can obtain the solution of Eqs. (13-15) – with realistic models – by direct recursion, i.e. by starting from a small initial energy interval and then calculating the number of particle in a final state for progressively growing initial energy.

Calculations of the Fano factor are presented in Fig. 6. The variation $F(E_0)$ follows the kinetic energy variance. Values of the Fano factor vary in the range from $F = 0.051$ to $F = 0.763$ depending on the model and grow further when the threshold energy is shifted to higher energy by the phonon emission.

The results of both the kinetic and the recursive approaches are supported by Monte Carlo modeling, in which one can exploit the fact (proven above) that in the final state the linear dependence on E_0 of both the average kinetic energy and its variance is exponentially accurate, starting from a reasonably small E_0 , certainly not exceeding $E_0 \approx 10 E_{th}$. As a result, both the average number of created pairs and its variance can be determined with Monte Carlo simulations with moderate values of E_0 . To be sure, in order to achieve the same accuracy as that obtained for large E_0 , the results must be averaged over a sufficient number of realizations. This, however, takes little memory or time.

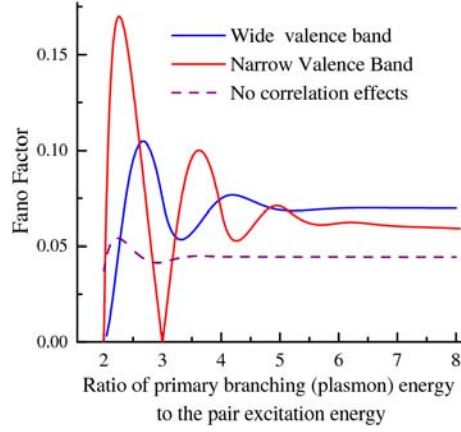


Figure 6. Fano factor dependence on the initial energy calculated recursively for a model with two symmetrical bands and for the case of a narrow valence band. Dotted line shows results obtained for the case of a narrow valence band in the final-state mode, using Eq. (5) with exact one-particle energy distribution function.

One can compare the computed values of the Fano factor with a hypothetical model in which the kinetic energy distribution of the particles in the final state is totally random within the interval $0 < E < E_{th}$. Since this distribution retains constant total energy for any number of pairs it can be viewed as a distribution of hard rods of length E_{th} along a segment of fixed total length E_0 . The random energy distribution should then be similar to the spatial distribution of particles shaped as hard rods in a one-dimensional gas (1D HR). For this problem one can calculate all multi-particle distribution functions,²³ which can be factored into products of pair correlation functions. The gaps in the 1D HR model are distributed in accordance with Poisson statistics, and F can be expressed in terms of the filling factor f (yield) exactly, viz. $F = (1 - f)^2$. In this model, there is no jamming limit and the filling factor can be as large as $f = 1$, but Eq. (3) is exact. The 1D HR model can also be modified to allow for two-band branching and the phonon shift of the E_{th} .

The 1D HR model is an attractive alternative to the shot-glass model, since in this model the one-particle distribution function is flat, but the main effect of the Fano statistics – the distribution of a constant initial energy between energies of the particles in the final state – is already exactly incorporated. Since, in contrast to the shot-glass model, the 1D HR model requires no additional assumptions about one-particle distribution, it can be viewed as a way to estimate the Fano factor for the known branching yield (the latter being determined by the pair excitation energy). For example, for a model of wide conduction and valence bands with square-root DOS, the yield is $f = 0.653$, giving $F = 0.120$. Inclusion of phonons further increases the Fano factor.

Consider the predictions of the 1D HR model for the exactly soluble RPP model. In this case, the jamming limit is exactly at $f = 0.74759\dots$ (the Rényi constant²³) and the predicted Fano factor is $F = 0.064$. It is clearly an upper bound to the exact RPP value $F = 0.051$.

5. Discussion and conclusion

Our analysis shows that the range of variation of the Fano factor with parameters of the material is not very broad. One can point out the features that would lead to an anomalously high value of the Fano factor, above $F = 0.1$. It is more intriguing to find such parameters that minimize the Fano factor. Our discussion suggests this may be achieved with a specially engineered alloy band structure, in which the valence band is either narrow or, which is more common, has sharp peaks in the density of states, so that the narrow valence band model becomes applicable. Correlation effects are more strongly pronounced in the narrow valence band limit. It would be most interesting to see some manifestation of the strong suppression of fluctuations by the correlation effects near $E_0 = 3 E_{th}$, illustrated in Fig. 4. One possibility would be to look for these effects in the dependence of noise in semiconductor X-ray detectors on the frequency $h\nu$ of incident X-ray flux of constant intensity. For $h\nu$ producing E_0 near $3E_{th}$ one can expect suppression of the noise component associated with the branching of energy of photoabsorbed quanta.

There is also a tantalizing possibility to employ these correlations in practical γ -detectors, where the energy is, of course much larger than $3E_{th}$. The possibility relies on the established fact that at high electron energies the dominant loss mechanism – up to the final stage of the branching process – is plasmon emission. This brings the initial energy (for the final stage of energy branching through the impact ionization cascade) close to the plasmon energy which is ≈ 16 eV in all common semiconductors. This energy is ≈ 4.5 times larger than the pair excitation energy ε for Si but only ≈ 3.5 times larger than that for CdZnTe and only ≈ 2.5 times larger than ε for GaP. Therefore, it is perhaps possible to find a compound crystal in which the ratio of the plasmon energy to E_{th} is optimal for the Fano factor reduction. The problem is not easy to handle theoretically with sufficient precision, because the threshold energy is based not only on the band structure but involves competition between phonon emission and impact ionization.

We conclude that correlation effects are important for the correct understanding of Fano statistics. Depending on the details of energy branching they can lead to either enhanced or suppressed value of the Fano factor and may be of value in the design of radiation detectors.

Acknowledgments

This work was supported by the Domestic Nuclear Detection Office (DNDO) of the Department of Homeland Security, by the Defense Threat Reduction Agency (DTRA) through its basic research program, and by the New York State Office of Science, Technology and Academic Research (NYSTAR) through the Center for Advanced Sensor Technology (Sensor CAT) at Stony Brook.

References

1. U. Fano , Ionization Yield of Radiations. II, “The fluctuations of the Number of Ions,” *Phys. Rev.* **72**, 26 (1947).
2. H. Spieler, *Semiconductor Detector Systems*, Oxford University Press, 2005.
3. L. Rossi, P. Fisher, T. Rohe, and N. Wermes, *Pixel Detectors: From Fundamentals to Applications (Particle Acceleration and Detection)*, Springer, Berlin (2006).
4. A. Kastalsky, S. Luryi, B. Spivak, “Semiconductor high-energy radiation scintillation detector,” *Nucl. Instr. Meth. Phys. Res.* **A 565**, 650 (2006).
5. C. E. Lehner, Z. He, and F. Zhang, “ 4π Compton imaging using a 3-D position-sensitive CdZnTe detector via weighted list-mode maximum likelihood,” *IEEE Trans. Nucl. Sci.* **51**, 1618 (2004).
6. S. Luryi, "Impregnated Semiconductor Scintillator", *International Journal of High Speed Electronics and Systems* **18**, 973 (2008).
7. R. Devanathan, L. R. Corrales, F. Gao, W. J. Weber, “Signal variance in γ -ray detectors – a review,” *Nucl. Instr. Meth. Phys. Res.* **A 565**, 637 (2006).
8. R.C. Alig, S. Bloom, C.W. Struck, “Scattering by ionization and phonon emission in semiconductors”, *Phys. Rev.* **B 22**, 5565 (1980).
9. J. Sempau, J. M. Fernandez-Varea, E. Acosta, F. Salvat, “Experimental Benchmarks Of The Monte Carlo Code Penelope,” *Nucl. Instr. Meth. Phys. Res.* **B 207**, 107 (2003).
10. M. Vilches, S. Garcia-Pareja, R. Guerrero, M. Anguiano, A. M. Lallena, “Monte Carlo simulation of the electron transport through thin slabs: A comparative study of PENELOPE, GEANT3, GEANT4, EGSnrc and MCNPX,” *Nucl. Instr. Meth. Phys. Res.* **B 254** 219 (2007).
11. H. Bichsel, “Straggling in thin silicon detectors”, *Rev. Mod. Phys.* **60**, 663 (1988).
12. D.V. Jordan, A. S. Reinolds, J.E. Jaffe, K.K. Anderson, L.R. Corrales, A. J. Peurrung, “Simple classical model for Fano statistics in radiation detectors,” *Nucl. Instr. Meth. Phys. Res.* **A 385**, 146 (2008).
13. C. Klein, “Bandgap dependence and related features of radiation ionization energies in semiconductors,” *J. Appl. Phys.* **39**, 2029 (1968).
14. H.R. Bilger, “Fano factor in Ge at 77 K,” *Phys. Rev.* **163**, 238 (1967).
15. W.E. Drummond, J.L. Moll, “Hot carriers in Si and Ge Detectors,” *J. Appl. Phys.* **42**, 5556 (1971).
16. A. Subashiev, S. Luryi, “Correlation effects in sequential energy branching: an exact model of the Fano statistics,” ArXiv: cond-mat/xxxxxxx; to appear in *Nucl. Instr. Meth. Phys. Res.* **A** (2010).
17. W. van Roosbroeck, “Theory of the Yield and Fano Factor of Electron-Hole Pairs Generated in Semiconductors by High-Energy Particles,” *Phys. Rev.* **139**, A1702 (1965).
18. A. V. Subashiev, S. Luryi, "Random sequential adsorption of shrinking or expanding particles," *Phys. Rev.* **E 75**, #011123 (2007).
19. A. V. Subashiev, S. Luryi, “Fluctuations of the partial filling factors in competitive RSA from binary mixtures,” *Phys. Rev.* **E 76**, #011128 (2007).

20. S. Picozzi, R. Asahi, C.B. Geller, A. Continenza, and A. J. Freeman, "Impact ionization in GaAs: A screened exchange density-functional approach", *Phys. Rev.* **B 65**, #113206 (2002).
21. Sh. Kogan, *Electronic noise and fluctuations in solids*, (Cambridge University Press, Cambridge, U.K., 1996)
22. A. Rényi, "On a One-Dimensional Problem Concerning Random Space-Filling." *Publ. Math. Inst. Hung. Acad. Sci.* **3**, 109 (1958).
23. Z. W. Salsburg, R. W. Zwanzig, J. G. Kirkwood, "Molecular Distribution Functions in a One-Dimensional Fluid", *J. Chem. Phys.* **21**, 1098 (1953).